

Self-Assembly of Amphiphilic Block Copolymers in Dispersions of Multiwalled Carbon Nanotubes As Reported by Spin Probe Electron Paramagnetic Resonance Spectroscopy

Rina Shvartzman-Cohen,[†] Ivonne Monje,[‡] Marc Florent,[‡] Veronica Frydman,[§] Daniella Goldfarb,^{*,‡} and Rachel Yerushalmi-Rozen^{*,†,§}

[†]Department of Chemical Engineering, Ben-Gurion University of the Negev, 84105 Beer Sheva, Israel, [‡]Department of Chemical Physics and [§]Chemical Research Support Unit, the Weizmann Institute of Science, 76100 Rehovot, Israel, and ^{*}The Ilse Katz Institute for Nanoscale Science and Technology, Ben-Gurion University of the Negev, 84105 Beer Sheva, Israel

Received September 1, 2009; Revised Manuscript Received December 9, 2009

ABSTRACT: Self-assembly (SA) of amphiphilic block copolymers (poly(ethylene oxide)–poly(propylene oxide)–poly(ethylene oxide)) was investigated in dispersions of multi-walled carbon nanotubes (MWNT) as a function of temperature using spin probe electron paramagnetic resonance (EPR) spectroscopy. Nitroxide-labeled Pluronic with a short poly(ethylene oxide) block, L62-NO, and a small molecular probe, 4-hydroxy-TEMPO-benzoate, 4HTB, were used for probing the local dynamic and polarity of the polymer chains in the presence of the nanostructures. It was found that MWNT modify the temperature, and the dynamic behavior of polymer SA and comparison between the MWNT and single-walled nanotube (SWNT) showed that the structure and dynamical behavior of the nanostructure–polymer hybrids formed depend on the size matching between the diameter of the native micelles and the additives. While SWNT induced the formation of hybrid polymer–SWNT micelles, MWNT (with a diameter of 20–40 nm) induced the assembly of polymer aggregates at the surface of the MWNT.

Introduction

Carbon nanotubes (CNTs) have attracted attention since their discovery due to their unique properties and potential applications. The excellent mechanical, electrical, and thermal properties^{1,2} of CNT may be utilized for preparation of advanced nanocomposite materials.^{2,3} A preferred preparation route for CNT-based materials relies on sonication-assisted dispersion of CNTs in a solvent, in the presence of a dispersing agent,⁴ often, a block copolymer.^{5–7} Among the most useful dispersing agents are the amphiphilic block copolymers poly(ethylene oxide)–poly(propylene oxide)–poly(ethylene oxide), PEO_yPPO_xPEO_y, (Poloxamers (ICI) or Pluronics (BASF)). Pluronic block copolymers are known⁹ to self-assemble (SA) in water into micelles consisting a hydrophobic core of PPO and a corona of the solvated PEO. Micellization is initiated (at a fixed temperature) by increasing the concentration to above a critical concentration, cmc, or by increasing the temperature (at a given concentration) to above a critical temperature, cmt.^{8,9}

It was shown^{10,11} that the structure and properties of hybrids formed in Pluronic–CNT dispersions differ from those of the native solutions. A thorough understanding of the mutual interactions from the molecular to the macroscopic level in these systems is an important prerequisite for the design of solvent-based preparation routes for nanocomposites. On the fundamental level, understanding of the mutual interactions among nanostructures and the block copolymers is of interest, as the dimensional match or mismatch between the components is expected to affect the phase behavior of the combined systems.^{10,11} While observations of SA in this system have been reported,^{11,12}

there are still many unresolved issues that need to be addressed experimentally before a complete characterization of these systems is achieved.

Few techniques have been used to provide a quantitative description of the microstructure of polymer–CNT dispersions. Transmission electron microscopy imaging, especially at cryogenic conditions,¹³ was found to enable structural characterization of the dispersed CNT.¹⁴ Yet the technique cannot provide the fine structure of the polymeric structures (micelles, aggregates) in cases where the mass contrast between the polymers and the vitrified liquid is not high enough.¹⁵ A limited number of scattering techniques, small-angle X-ray, neutron, and light scattering with wave vectors in the range 10^{-3} – 10^2 nm⁻¹ (corresponding to length scales 1–1000 nm), were used to investigate CNT assembly in polymeric (and surfactant) dispersions.^{16,17} These methods rely heavily on the assumed rigid-rod behavior of single-walled carbon nanotubes (SWNT),¹⁶ and the interpretation of the results is still debated in the literature. Moreover, these methods do not provide detailed information about the phase behavior of the dispersing polymer. The interpretation of the results is even more troublesome in the case of multi-walled carbon nanotubes (MWNT) that are highly flexible with typical diameters between 10 and 80 nm.¹⁸

As was shown before,¹¹ the microscopic details of the assembly of amphiphilic block copolymers in aqueous dispersions of MWNT and SWNT may be probed by spin-probe electron paramagnetic resonance (EPR) spectroscopy. Spin-probe EPR spectroscopy is a well-established method: nitroxide spin-labels are introduced into systems where no paramagnetic center is present. The EPR spectrum of the spin-label reflects the properties of their local environment and provides information on their motional characteristics in terms of rotational correlation times and order parameter.¹⁹ Moreover, the polarity of a spin-label's

*Corresponding authors. E-mail: daniella.goldfarb@weizmann.ac.il (D.G.); rachely@bgu.ac.il (R.Y.-R.).

microenvironment can be probed by the isotropic ^{14}N hyperfine coupling, a_{iso} , which decreases when the polarity of the environment decreases¹⁹ and therefore can be used to detect processes such as micellization²⁰ as long as they are associated with a change in polarity and mobility.

In a previous study^{11,12} we used two Pluronic-based spin probes to investigate the temperature-dependent SA in Pluronic dispersions of SWNT. In these probes a nitroxide label is covalently linked at each of the two end-groups of the PEO moieties and thus reports the more hydrophilic PEO-rich regions of the system. A major issue in any probe-based technique²² is the affinity of the probe to specific moieties comprising the investigated system. If present, it excludes a general overview of the system. In our system, the nitroxide end-groups covalently linked to the PEO moieties in the Pluronic-based spin probes affect the hydrophobic/hydrophilic balance of the probe chains. Thus, one should examine their effect on the tendency of the labeled molecules to incorporate into the polymeric micelles and the possibility of selective interaction of the nitroxide end-groups with the nanostructures.²² To test these and other specific effects of the NO end-groups on the SA system, we carried out control experiments. In these experiments PEO chains end-terminated by covalently linked nitroxide spin-labels were used as probes. Our findings indicate that the nitroxide group does not lead to incorporation of PEO chains into forming micelles, does not affect the transition to micelles, nor does it interact specifically with the micelles or the CNT.

To probe the PPO block, which is the one interacting with the hydrophobic CNT,²³ we used a nitroxide-labeled Pluronic (L62) with a short PEO block, L62-NO, where the label resides close to the dehydrated PPO core of the Pluronic micelles^{24,25} and a small molecular probe, 4-hydroxy-TEMPO-benzoate (4HTB). The latter is known to reside in the hydrophobic region of the micelles.^{24,25} Comparison between the molecular information provided by the two probes, (Pluronic-based and 4HTB) at different temperatures, enables us to investigate the detailed behavior of the polymers at the interface of the two nanostructures. We find that the micellization of Pluronic block copolymers is sensitive to the presence of nanostructures and depends on their sizes. While a good size-matching between the diameter of the native micelles (about 8 nm) and the additives (1–2 nm for SWNT) results in combined SA, size mismatch leads to a distinct behavior. Indeed, SA at the surface of MWNT (with a diameter of 20–40 nm) is different from SA of the polymer–SWNT systems and resembles the behavior observed at the surface of colloidal particles.²¹

Experimental Section

Materials. Polymers. P123 Pluronic triblock copolymer (PEO₂₀–PPO₇₀–PEO₂₀) [$M_w = 5750$, cat. no. 587440] was received as a gift from BASF AG Germany and used as received.

Carbon Nanotubes. Raw SWNT synthesized by arc discharge were purchased from Carbolex Inc. (<http://carbolex.com>) and used as received. According to the specifications by the manufacturer, the as-prepared AP grade consists of 50–70 vol % SWNT as well as graphite and the carbonated catalyst. MWNT produced by catalytic chemical vapor deposition were purchased from INP, Toulouse, France. The powder contains 95 vol % MWNT, and the tube diameters are above 20 nm with lengths of micrometers and specific areas of 700–1000 m²/g.

Spin Probes. Spin-labeled Pluronics P123-NO (Supporting Information) and L62-NO (PEO₆–PPO₃₆–PEO₆) and two different lengths of PEO-NO (PEO-10K [PEO2OH-10K] and PEO-0.6K [PEG2OH-0.6K] from Polymer Source) were synthesized as described in the literature.²² The spin-label is covalently attached to the terminal hydroxyl chains. 4HTB (4 hydroxy-TEMPO-benzoate) was purchased from Aldrich [cat. no. 371343].

Sample Preparation. Aqueous solutions of the block copolymers were prepared by dissolving a block copolymer in water at room temperature (22–24 °C) to form solutions of desired wt %. The solutions were mixed for about 2 days using a magnetic stirrer. An appropriate volume of a 5–10 mM stock solution of the spin probe in ethanol was added to a vial, and the solvent was evaporated. Then, an appropriate volume of an aqueous Pluronic solution was added, and the sample was stirred overnight to ensure complete dissolution of the spin probe to a final concentration of 0.1–0.5 mM (equivalent to 1 spin probe molecule per 7–15 polymer molecules). Liquid dispersions of CNT were prepared following the previously published procedure:^{14,26} 1 wt % of the raw material was sonicated at mild conditions (50 W, 43 kHz) for 30–40 min in a polymeric solution (containing the spin probe). The dispersions were centrifuged (at 4500 rpm for 30 min), and the supernatant was decanted from above the precipitate. As was shown before,²⁶ the dispersion process is selective toward CNT, and the precipitate mainly contains colloidal moieties; thus, the actual concentration of dispersed CNT is somewhat lower than the initial concentration of CNT powder. The relative concentrations of dispersed CNT and dissolved polymeric molecules were modified by two different procedures: (1) Stock dispersions of CNT in 1 wt % of P123 containing 0.1–0.5 mM spin probe were prepared. A known volume of 1 wt % polymer solution (containing spin probes at the required ratio) was added to the stock dispersion, resulting in a dispersion of a lower CNT concentration at a fixed polymer concentration. (2) In a different set of experiments the polymer–CNT ratio was modified by increasing the overall polymer concentration, while keeping the concentration of the CNT constant. In this route a polymer powder was dissolved in the stock dispersion up to the final polymer concentration.

Techniques and Methods. Spin Probe EPR. EPR spectra were recorded using a modified Varian B-12 X-band spectrometer or a Bruker Elexsys 500 spectrometer. Modulation amplitude of 0.03 mT was used. The samples were placed in a glass capillary, and the temperature was controlled using the spectrometer temperature controller. For temperatures lower than room temperature the sample was cooled by N₂ gas passing through an acetone/dry ice bath. The actual temperature was determined independently by a thermocouple located at the center of the cavity. Spectra were recorded while increasing and decreasing the temperature, with equilibration periods of 15 min between each step. Comparison of the heating and cooling sequences showed that the measurements are reversible and do not exhibit hysteresis.

The measured EPR spectra were all in the fast limit region. When only one species is present in solution, the correlation time, τ_c (in s), is derived from the relative intensities and width of the individual hyperfine components according to the relation²⁷

$$\tau_c = (6.51 \times 10^{-10}) \Delta H(0) \{ [h(0)/h(-1)]^{1/2} + [h(0)/h(1)]^{1/2} - 2 \} \quad (1)$$

where $\Delta H(0)$ is the peak-to-peak line width (in mT) of the central line of the nitroxide spectrum and $h(-1)$, $h(0)$, and $h(1)$ are the peak-to-peak heights of the $M_I = -1$, 0, and +1 lines, respectively. An experimental error of 0.02 mT was derived from the line width of the peaks at three different locations. When two species contribute to the EPR spectrum, their relative contributions, a_{iso} and τ_c values, were determined from simulations using least-squares fitting of the spectra. The program used was “garlic” of the Easyspin software package.²⁸ We simulated each component S_i and S_m individually and added them using a ratio factor. The line shape used was Lorentzian. The program “garlic” is applicable for fast motion and assumes an isotropic tumbling that is governed by a Brownian movement. The speed of tumbling is determined by the rotational correlation time. The error was determined from the range of the parameters (a_{iso} , τ_c) that produced similar qualities of fits.

Cryo-TEM. Solutions of Pluronic block copolymers that contain dispersed MWNT and SWNT were characterized via direct imaging of the dispersions using cryo-transmission electron microscopy.¹³ Sample preparation for cryo-TEM measurements was carried out as follows: a drop of the solution was deposited on a TEM grid (300 mesh Cu grid) coated with a holey carbon film (Lacey substrate-Ted Pella Ltd.). The excess liquid was blotted, and the specimen was vitrified, by a rapid plunging into liquid ethane precooled with liquid nitrogen, in a controlled environment vitrification system. The samples were examined at $-178\text{ }^{\circ}\text{C}$ using a FEI Tecnai 12 G² TWIN TEM equipped with a

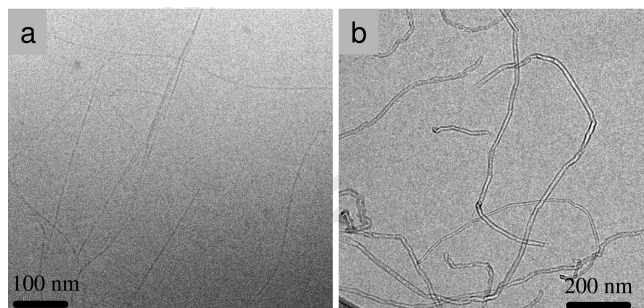


Figure 1. Typical cryo-TEM images of CNT dispersions in P123 (1 wt %) with 0.5 mM L62-NO: (a) SWNT (0.5 wt %) and (b) MWNT (0.5 wt %).

Gatan 626 cold stage, and the images were recorded (Gatan model 794 CCD camera) at 120 kV in low-dose mode.

Results

Dispersions of MWNT and SWNT in aqueous solutions of 1 wt % P123 were prepared following a previously published procedure.^{26,14,5} In Figure 1, we present a cryo-TEM image of MWNT and SWNT in P123 dispersions. As was previously reported by us, the formed dispersions are stable and long-lived.^{26,5} Cryo-TEM suggests that the most abundant species in similar dispersions are individual tubes (and small bundles of SWNT).

Control Experiments: PEO-NO. PEO-NO of two different molecular weights, PEO-10K (~ 200 monomers) and PEO-0.6K (~ 12 monomers), were used to test the effect of the nitroxide end-groups on the system and exclude the presence of specific interactions between the spin-label and CNT. The spin probes were mixed with P123 (PPO = 70, PEO = 40 monomers) solutions of 1 and 4 wt %, at concentrations of 0.3–0.5 mM. In Figure 2 we present the temperature dependence of the EPR spectra of the PEO-NO (0.5 mM) probes in an aqueous solution of P123 (1 wt %). From the EPR results it is evident that PEO-NO does not detect a micellization process and that the rotational correlation time of both PEO-NO probes is reduced with the temperature, as expected for a dissolved polymer, while a_{iso} remains fairly constant. We note that at this temperature regime water is a moderately

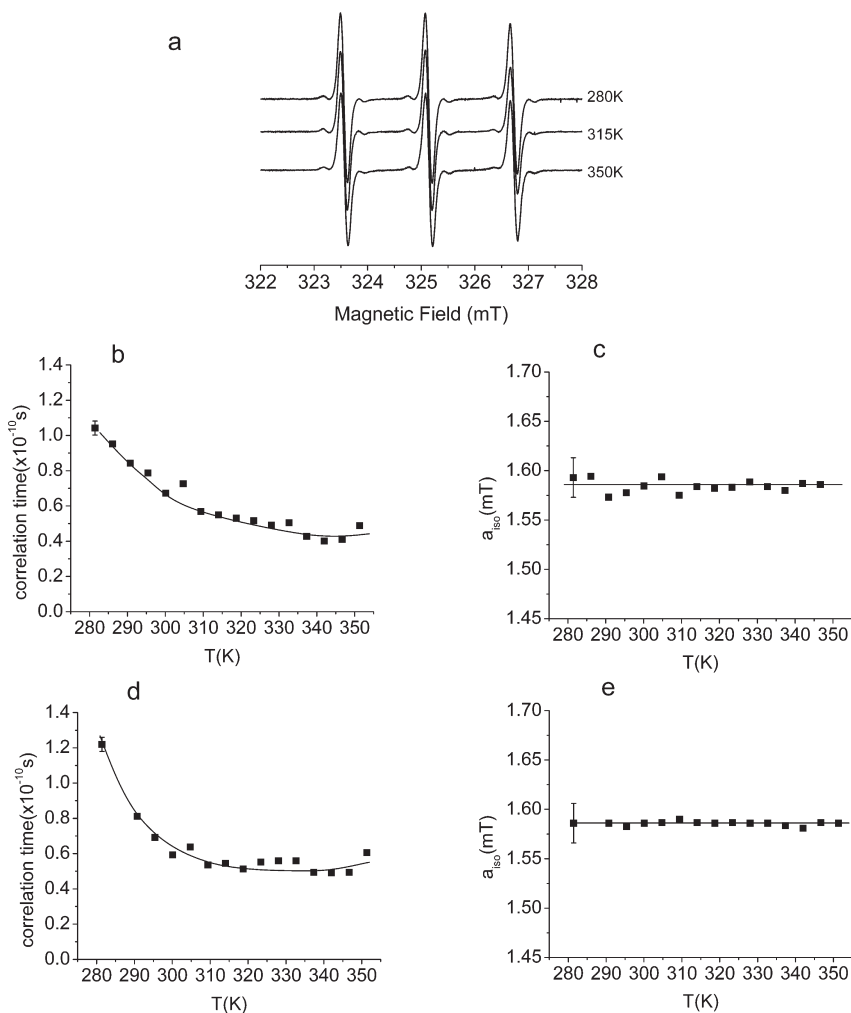


Figure 2. Temperature dependence of the EPR spectra of two PEO-NO spin probes in aqueous solutions of P123 (1 wt %). PEO-10K-NO (0.5 mM): (a) EPR spectra as a function of temperature (b) τ_c and (c) a_{iso} ; PEO-0.6K-NO (0.5 mM): (d) τ_c and (e) a_{iso} . The lines are guides to the eye. An error bar is displayed for one representative point.

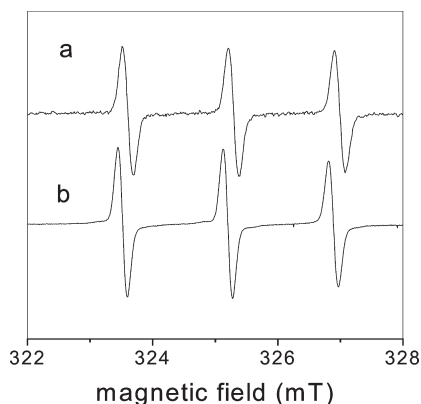


Figure 3. EPR spectra of 4HTB in (a) water and (b) a 1 wt % solution of P123 in water ($T = 290$ K).

good solvent for the PEO.²⁹ A similar result was observed for a higher concentration (4 wt %) of P123. Thus, while the nitroxide labeled Pluronic, P123-NO, clearly detect the micellization process, with an abrupt change in the values of a_{iso} and τ_c during the transition,¹² the PEO-NO does not.

The fact that the spin probe is not involved in the micellization process and remains solvated in water suggests that the nitroxide does not interact specifically with the micelles and thus does not affect the transition.

An additional set of measurements was carried out using these PEO-NO spin probes in dispersions of SWNT and MWNT to examine the possible interactions of the nitroxide group with the CNT. These measurements, shown in the Supporting Information, clearly indicate that the PEO-NO probe does not adsorb onto CNT.

SA in Native Solutions of P123 and CNT Dispersions As Reported by 4HTB. 4HTB is a hydrophobic molecule which is soluble in water in minute concentrations and readily dissolves in aqueous solutions of an amphiphilic block copolymer such as Pluronic. EPR spectra of 4HTB in water and in solutions of P123 (below cmt) are very similar (see Figure 3), except for the increase in signal-to-noise that indicates that 4HTB adsorbs onto the polymer chain and the amphiphilic polymer acts as a solubilizing agent for the hydrophobic 4HTB.

As shown by Ruthstein et al.²⁰ and schematically presented in Figure 4b,c above cmt 4HTB probes the PPO-rich core of the Pluronic micelles.

This observation suggests that 4HTB may be used to probe the local environment of the PPO region and therefore provides complementary information to that provided by the Pluronic-based spin probes that mainly probe the PEO region of Pluronic micelles.^{11,12,20}

In Figure 5 we present the temperature dependence of the EPR spectra of 4HTB (0.5 mM) in aqueous solution of P123 (1 wt %). Micellization is identified by a reduction in a_{iso} and a broadening of the line width. At the onset of the transition (and at temperatures above) two species are observed, differing in their a_{iso} and τ_c values, referred to as S_m and S_i . The temperature dependence of the relative concentrations of the two species and that of τ_c and a_{iso} are shown in parts b, c, and d of Figure 5, respectively. S_m and S_i are distinguishable on the EPR time scale up to 355 K, with a ratio of 80% S_m to 20% S_i at the highest measured temperature of 355 K. There is a clear difference between τ_c and a_{iso} values of the two species, with lower a_{iso} values and higher τ_c for the S_m species. This observation is consistent with the decreased rotational correlation mobility and lower polarity within the micelles.²⁰ Accordingly, S_m is assigned to 4HTB in micelles and S_i to 4HTB dissolved by individual polymer chains. We

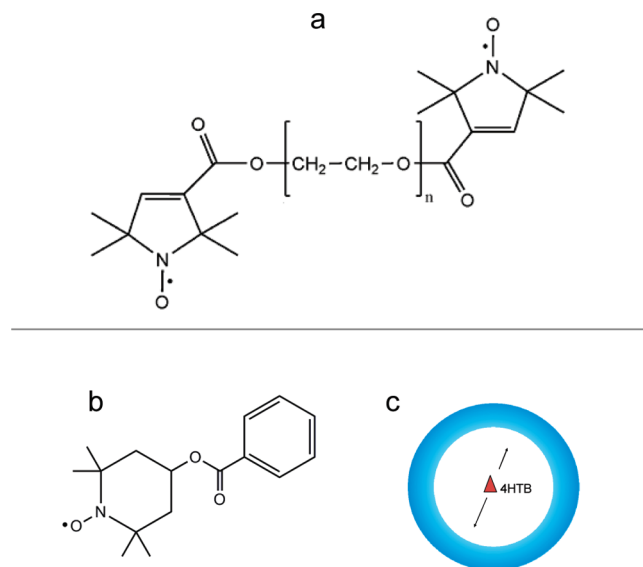


Figure 4. Molecular structures of the spin probes used: (a) PEO-NO, (b) 4HTB, and (c) a schematic representation locating the 4HTB molecule within the hydrophobic core of Pluronic micelle, following refs 20 and 21.

observe that 4HTB reports a negligible change in τ_c and a_{iso} for S_i as a consequence of micelles formation.

The temperature dependence of a_{iso} and τ_c of 4HTB in P123 dispersions of MWNT is presented in Figure 6. As in the native solution, we observe the onset of micellization and the appearance of two distinguishable populations, S_i and S_m . Micelles are first detected at 305 K, and a broad micellization transition of about 20 K is observed. Note that the temperature range over which the relative concentration of micelles grows is much wider than in the native solutions. Further, in the presence of MWNT 35% of the spin probe molecules reside in the aggregates (S_m), a significantly lower fraction compared to the native solution. The temperature dependence of a_{iso} is similar to that observed in the native solutions, and higher τ_c values for MWNT dispersions indicate lower rotational mobility of the spin probes.

In Figure 7 we present the temperature dependence of a_{iso} and τ_c of 4HTB (0.5 mM) in aqueous dispersions of SWNT (1 wt %) in P123 (1 wt %) as a function of temperature. Here again a broad micellization transition is detected over ~ 20 K (onset at 295 K). After the transition the majority of the 4HTB molecules are located in the micellar aggregates with $S_m:S_i = 63\%:37\%$. The significant temperature dependence of τ_c within the S_m environment at the temperature range of 305–345 K follows the Arrhenius law yielding an activation energy of ~ 8.5 kJ/mol (see Figure S2 in Supporting Information).

SA in Native Solutions of P123 and CNT Dispersions As Reported by L62-NO. EPR spectra of L62-NO (0.1 mM) in P123 (1 wt %) dispersions of MWNT as a function of temperature are presented in Figure 8. We observe that the onset of the micellization is slightly shifted as compared to the native solution¹¹ (Figure 8a: 310 K instead of 300 K). Again, two species are present above cmt with $S_m:S_i \sim 82\%:18\%$. The temperature dependence of τ_c is similar to that observed for 4HTB.

The temperature dependence of τ_c is similar to that reported previously^{11,12} for SWNT dispersions in P123 (1 wt %): τ_c does not change much with temperature, while the absolute values are slightly higher for MWNT ($\sim 6.5 \times 10^{-10}$ s at 345 K) as compared to SWNT ($\sim 4.5 \times 10^{-10}$ s at 345 K¹²). The ratio of S_m and S_i is however different for

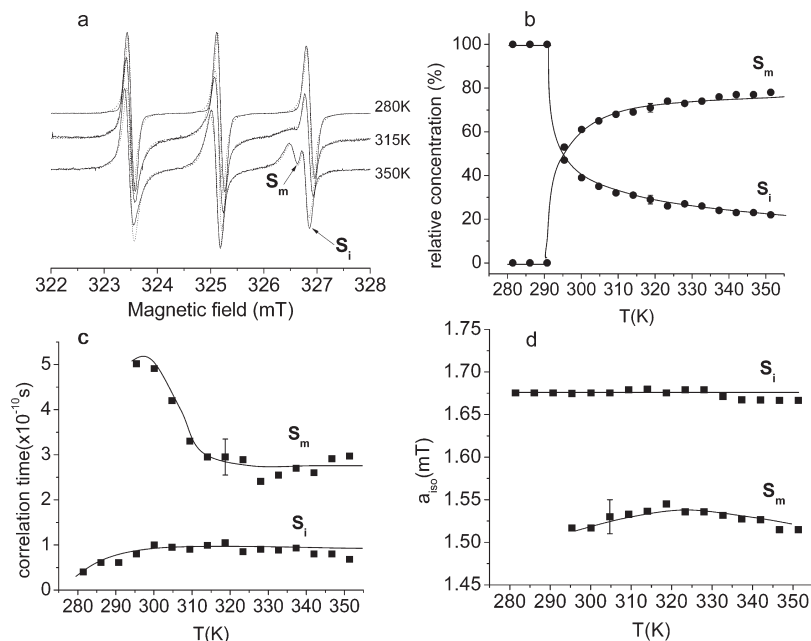


Figure 5. EPR spectra of 4HTB (0.5 mM) as a function of temperature in aqueous solution of P123 (1 wt %). (a) Sample EPR spectra at different temperatures with their simulations (dotted lines) obtained with parameters shown in (b), (c), and (d) at the relevant temperatures. (b) Temperature dependence of the relative concentrations of S_i and S_m , (c) τ_c , and (d) a_{iso} . The lines are guides to the eye. An error bar is displayed for one representative point.

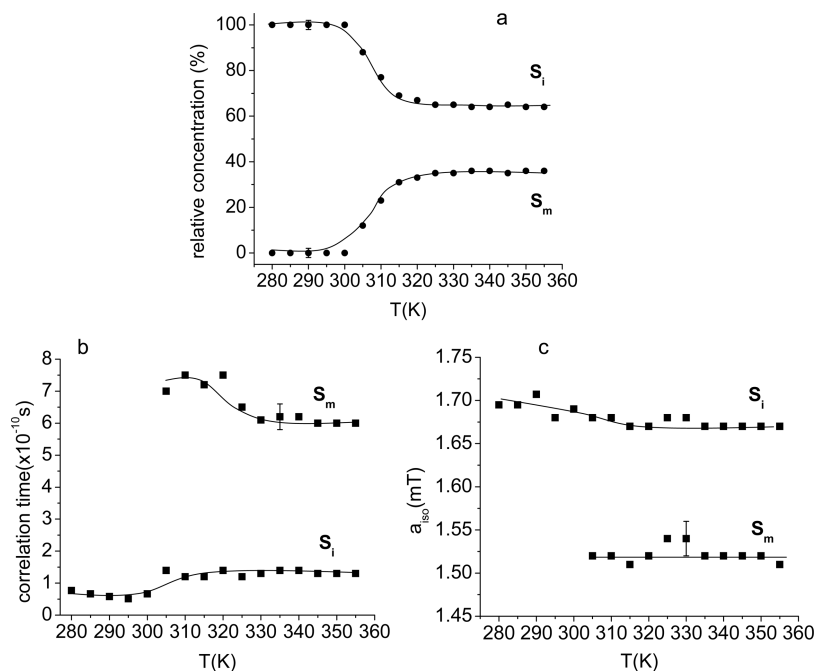


Figure 6. The temperature dependence of (a) the fraction of S_i and S_m (b), τ_c and (c) a_{iso} of 4HTB (0.5 mM) in aqueous dispersions of MWNT (1 wt%) in P123 (1 wt%). The jump in S_i in (b) at ~ 305 K is an artifact of the simulation. The lines are guides to the eye. An error bar is displayed for one representative point.

dispersed MWNT. This change, however, can be due to different actual concentration of the dispersed CNTs and not their character. This issue is addressed later.

To obtain complementary information, we also used a spin probe of a longer PEO chain, P123-NO. Unlike the 4HTB and the L62-NO probes, the P123-NO resides in the PEO-rich region of the micelle. We found that this probe reports a complete transition from individual chains (S_i) to aggregated chains (S_m), both in the native solutions and in the presence of the dispersed MWNT (while two species were detected in SWNT dispersion^{11,12}) (see Supporting Information).

Quantitative comparison of the $S_m:S_i$ ratio in different samples relies on the ability to control the absolute concentration of dispersed CNT. Yet, the absolute concentration may vary between different samples, while a reliable quantitative measure of the absolute concentration of dispersed CNT is not yet available.³⁰ To overcome this issue and obtain further information regarding trends of the partitioning of two spin probes, L62-NO and 4HTB, between the two environments, we modified the CNT-polymer ratio in two distinct ways. In the first set of experiments the concentration of P123 in the aqueous solution

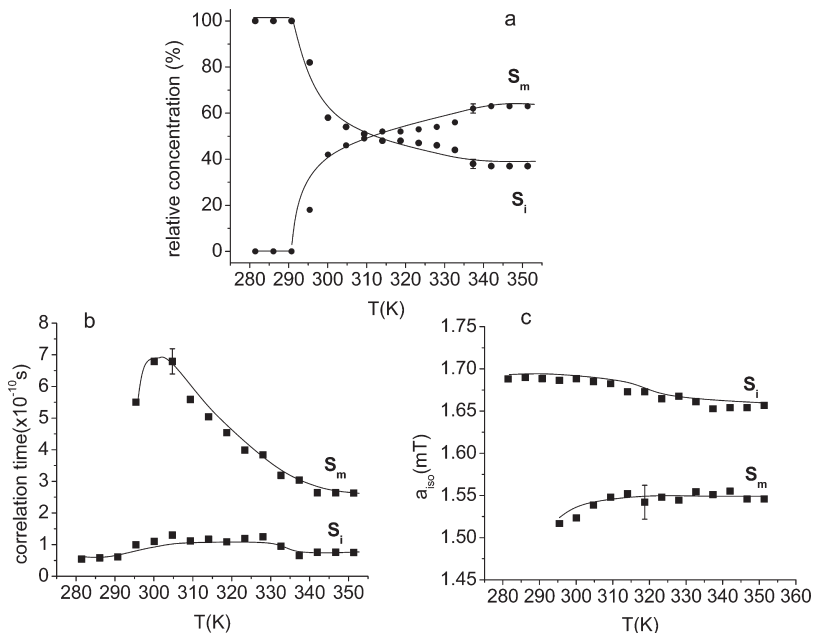


Figure 7. The temperature dependence of (a) the fractions of S_i and S_m (b) τ_c and (c) a_{iso} of 4HTB (0.5 mM) in aqueous dispersions of SWNT (1 wt%) in P123 (1 wt%). The lines are guides to the eye. An error bar is displayed for one representative point.

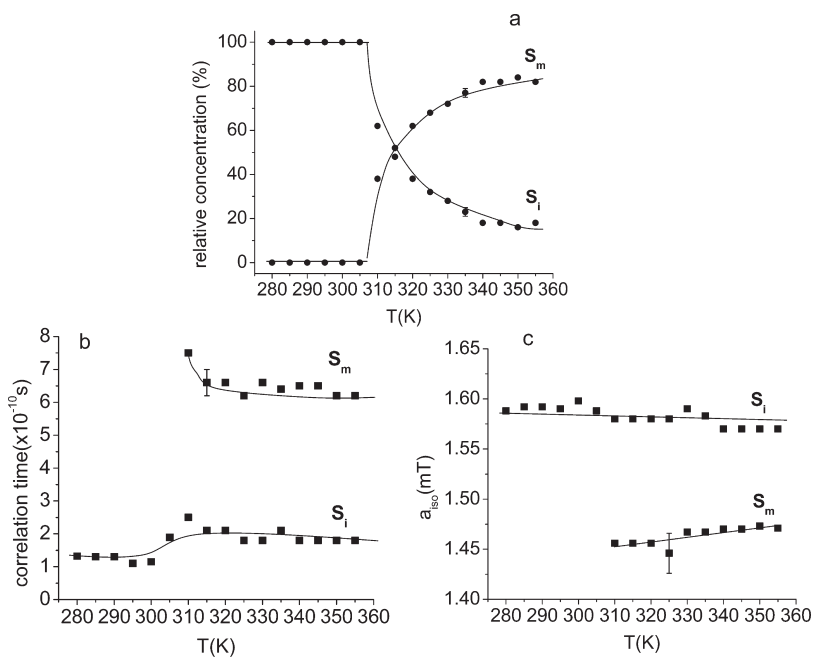


Figure 8. The temperature dependence of (a) the fraction of S_i and S_m (b) τ_c and (c) a_{iso} of L62-NO (0.1 mM) in aqueous dispersions of MWNT (1 wt%) in P123 (1 wt%). The lines are guides to the eye. An error bar is displayed for one representative point.

was kept constant, while the concentration of dispersed CNT was reduced by increasing the volume of the polymer solution. In the second set of experiments the concentration of P123 was increased by dissolution of additional solid polymer in the preprepared dispersion, thus keeping the concentration of CNT constant. EPR spectra were recorded in solutions of P123 above the cmt (at 345 K), using the two different spin probes. A systematic comparison of the values of S_i in SWNT and MWNT dispersions is presented in Figure 9. Figures 9a,b present the value of S_i as a function of CNT wt % measured in dispersions of P123 of a fixed P123 concentration (1 wt %). Figures 9c,d present the values of S_i in dispersions comprising of a fixed concentration of CNT (1 wt %) as a function of P123 concen-

tration. Note that Figures 9a,c report the observations of the 4HTB probe while Figures 9b,d report results obtained from the L62-NO probe.

The spectra clearly show that as the relative concentration of CNT increases (Figures 9a,b), the fraction of S_i increases, apart from the case of SWNT as reported by 4HTB (Figure 9a). This result suggests that as more interfaces are available to the adsorbing molecules, single-molecules adsorption is preferred over aggregation. While the behavior is general, the absolute values and the slopes of the graphs depend on the nanoadditive as well as on the reporting probe. The (almost) constant fraction of S_i in the case of SWNT reported by 4HTB is discussed in detail in the Discussion section.

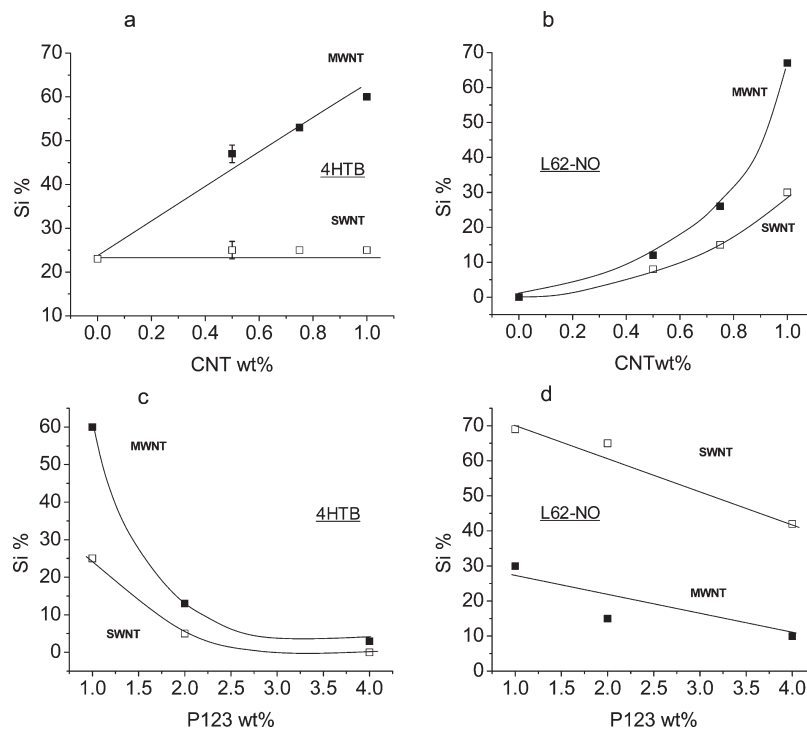


Figure 9. Fraction of S_i as a function of CNT concentration at P123 (1 wt %) for (a) 4HTB and (b) L62-NO spin probes and as a function of P123 concentration at CNT (1 wt %) using (c) 4HTB and (d) L62-NO spin probe. An error bar is displayed for one representative point.

Table 1. Values of a_{iso} and τ_c in Dispersions of CNT (1 wt %) in P123 Solutions (1 wt %) Using Different Spin Probes, Compared to the Native Solutions ($T = 345$ K)

sample		S_i		S_m	
		a_{iso} (mT)	$\tau_c (\times 10^{-10} \text{ s})$	a_{iso} (mT)	$\tau_c (\times 10^{-10} \text{ s})$
4HTB (0.5 mM) in P123 (1 wt %)	0% CNT	1.67 ± 0.02	0.8 ± 0.4	1.51 ± 0.02	2.8 ± 0.4
	SWNT 1 wt %	1.65 ± 0.02	0.8 ± 0.4	1.54 ± 0.02	2.6 ± 0.4
	MWNT 1 wt %	1.67 ± 0.02	1.3 ± 0.4	1.51 ± 0.02	6.2 ± 0.4
L62-NO (0.1 mM) in P123 (1 wt %)	0% CNT ¹²			1.48 ± 0.02	2.3 ± 0.4
	SWNT 1 wt % ¹²	1.62 ± 0.02	1.4 ± 0.4	1.38 ± 0.02	4.5 ± 0.4
	MWNT 1 wt %	1.57 ± 0.02	1.8 ± 0.4	1.47 ± 0.02	6.5 ± 0.4

Figures 9c,d report that as the concentration of the dispersing polymer is increased (while the CNT concentration is preserved), aggregation (or micellization) takes place and thus the overall fraction of the individual molecules (S_i) is reduced; while the tendency is similar for both SWNT and MWNT and the two spin probes, the detailed dependence on the concentration of the polymer depends on the details of the system.

Discussion

In this study we utilized two spin probes for molecular level characterization of the temperature-induced SA of Pluronic block copolymers at the interface between hydrophobic CNT and an aqueous solution. We used 4HTB, a small hydrophobic molecule, and a nitroxide-labeled Pluronic triblock copolymer L62-NO. These spin probes differ in their hydrophobicities and dimensions and are thus expected to provide complementary information with respect to the behavior of the hydrophilic and hydrophobic regions of the self-assembled structures. Using a set of control experiments, we established the absence of specific interactions between the nitroxide spin-label and the different components of the polymer–CNT dispersions.

We find that the presence of CNT modifies the aggregation and SA of Pluronics in aqueous dispersions, affecting the dynamics and the partitioning of the probes between aggregates (S_m) and free chains (S_i). In Table 1 we summarize the

information reported by the two different spin probes on the Pluronic SA in the presence of dispersed MWNT and SWNT. L62-NO reports that the aggregates formed in CNT dispersions are characterized by higher τ_c values as compared to those of the (native) micellar solutions, with those on the MWNT being the slowest, indicating that the aggregates formed at the surface of the CNT. This observation suggests that chains adsorbed onto the MWNT surface suffer from steric hindrance. The observation of a single micellar species (within our experimental resolution) indicates that only one type of micelles is present. This suggests that free polymer micelles are not present and aggregation only takes place on the surface of the dispersed CNT. However, we cannot exclude the possibility that they cannot be resolved with our method. The 4HTB probe reports a behavior that is similar in micelles formed in the native solutions and the SWNT dispersion, whereas a significant motional slowdown is observed for aggregates formed on the MWNT.

The temperature variation of the EPR spectra of the two probes enables us to characterize the dynamic behavior of the CNT–Pluronic systems. Following the formation of micelles, we observe that in the presence of SWNT and MWNT the aggregates do not show the typical increase in mobility as a function of temperature (Figures 6 and 8) observed in the post-cmt regime of the native Pluronic micelles.^{11,12} A unique behavior is reported by 4HTB in SWNT dispersions, where the rotational mobility of the aggregates in the dispersion and the native

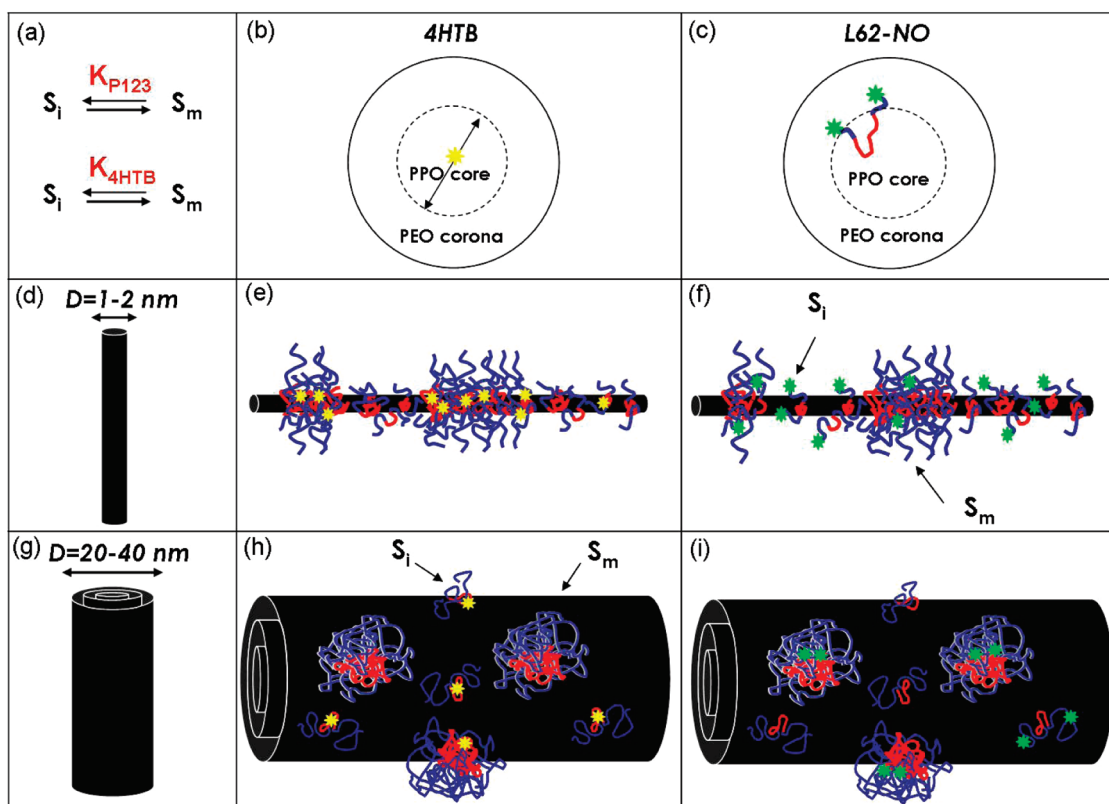


Figure 10. A schematic summarizing the findings: (a) partitioning of the spin probe molecules, (b) 4HTB (yellow stars), and (c) L62-NO (green stars) between aggregates (S_m) and single chains (S_i) is affected by the dimensions of the nanostructure and the nature of the spin probe: The match or mismatch between the dimensions of the CNT and the native polymer micelles plays a crucial role in the interaction: While (d), (e), and (f) SWNT present a minor disturbance to the micellization of the polymers (g), (h), and (i) MWNT present a significant disturbance to the adsorbed chains and affect their dynamics. The formation of a new type of micrometer-long cylindrical aggregates where a SWNT is located at the core of the aggregate is suggested by the spectra of the two spin probes ((e), (f)), and aggregation of “surface micelles” like structures at the surface of MWNT ((h), (i)).

micelles are more similar than with MWNT, indicating that the presence of the SWNT does not affect the behavior of the dissolved 4HTB. Here activation energy of ~ 8.5 kJ/mol was obtained for the motion of 4HTB within the micelles; this value is in the range reported for CTAB micelles.³²

4HTB reports a broad aggregation transition (Figures 6 and 7) in the presence of CNT, while the nitroxide-labeled Pluronic spin probes^{11,12} do not experience similar broadening in CNT dispersions. We suggest that the broadening of the transition in the case of 4HTB is related to its ability to probe the appearance of intermediate species (with different affinities) both adsorbed on the CNT and in solution. Its high mobility enables the 4HTB molecule to sample different environments, each characterized by a different correlation time, that form during the transition. The polymeric spin probes, on the other hand, are irreversibly (on the EPR time scale) adsorbed onto the CNT as was shown before¹² and are thus insensitive to transient assemblies in the solution.

Above the transition, the system equilibrates into two distinguishable species S_m and S_i . As we have shown before^{11,12} in CNT dispersions S_m represents aggregates that are formed on the dispersed moieties. Comparison between the τ_c values of the S_m species in SWNT dispersions and τ_c values of aggregates formed in MWNT dispersions suggests that while SWNT have a minor effect on the dynamics of the aggregated polymers, MWNT have a significant effect. Indeed, as presented schematically in Figure 10, and was suggested by us before,^{11,12} the significant dimensional mismatch between the MWNT (where $d > 20$ nm) and the polymeric micelles ($d \sim 8$ nm⁹) results in a significant geometrical perturbation to the hydrophobic core of the polymer micelles. Thus, while polymeric aggregates may adsorb on the MWNT, they do not incorporate the tube into the core and do

not form an elongated-micelle-like structure, as suggested in the case of SWNT (Figure 10). An additional insight is provided by the rationalization of the ratios of the two populations and their dependence on the CNT/P123 ratio (see Figure 9). In the case of L62-NO, which is a block copolymer, the presence of CNT results in an increase in the relative amount of S_i for both SWNT or MWNT, showing that the partitioning equilibrium constant, K_{P123} , of the polymer molecule between aggregates and single chains is affected by the CNT surface area, namely K_{P123} decreases (see Figure 10). The increase of S_i is steeper for MWNT because of its larger surface area. Increasing the relative concentration of P123 reduces S_i , as expected; again, the slope is milder for MWNT (Figure 9d).

The behavior of 4HTB in the presence of MWNT is in general similar to that of L62-NO; as the relative concentration of CNT increases, the fraction of S_i increases. The increase is linear and milder than for L62-NO. Assuming that the behavior of L62-NO represents that of the native P123, this suggests that the addition of MWNT affects K_{4HTB} (see Figure 10) differently than K_{P123} such that K_{P123}/K_{4HTB} (MWNT) is slightly smaller than K_{P123}/K_{4HTB} (free). Namely, the addition of MWNT leads to a small preference of 4HTB to the aggregates (Figure 10). In the case of SWNT, the $S_m:S_i$ ratio is constant while the equilibrium partitioning of Pluronic spin probe (and Pluronic native molecules) shifts toward S_i (Figure 10) as CNT are added. This indicates that for SWNT the affinity of 4HTB to the aggregates increases significantly more than for MWNT, namely K_{P123}/K_{4HTB} (SWNT) $<$ K_{P123}/K_{4HTB} (MWNT) (see the equilibrium equation in Figure 10).

A question that arises is what is the origin of the larger affinity of 4HTB to the aggregates in SWNT as compared to MWNT?

Here again the key feature is the combination of the hydrophobicity of the surfaces and their dimensions: while SWNT–Pluronic micelles present a core which is similar though somewhat more hydrophobic than the native Pluronic core, the Pluronic–MWNT interface is both more hydrophobic and more dense. As was shown before,³¹ 4HTB is expelled from such an environment, and thus its affinity to the core is reduced.

The distinguished natures of 4HTB and the Pluronic spin-labels expose different properties of the investigated system. While L62-NO emphasizes the effects of the CNT dimensionality on the SA, namely the ratio between single adsorbed chain and adsorbed aggregates, 4HTB could probe differences in the properties of the core of the adsorbed aggregates.

Conclusions

The utilization of EPR for the investigation of the molecular details of self-assembling systems and in particular complex systems such as amphiphilic block copolymers in dispersions of nanostructures is very promising. Utilization of probes that differ in their hydrophobicity and size (small molecules vs polymers) enables one to detect different properties of the system. Systematic characterization of the self-assembly of Pluronic block copolymers in dispersions of CNT reveals that CNT affect the temperature induced self-assembly of Pluronic block copolymers in aqueous solutions and result in the formation of two distinct types of hybrids—SWNT: polymer elongated-micelle-like structures; MWNT: decorated by “surface micelles”. We find that dimensional mismatch between MWNT and the native polymer micelles MWNT results in a significant disturbance to the adsorbed chains and affects their dynamics. The suggested model is consistent with our previous study of SWNT^{11,12} and highlights the effects of dimensionality on SA in hybrid systems of nanostructures and polymers, where unique features emerge from the nanometric dimensions of the investigated structures.

Acknowledgment. R.Y.-R. and D.G. thank the Israel Science Foundation. R.S.-C. acknowledges the support of the Eshkol scholarship program of the Israel Ministry of Science and Technology. D.G. holds the Erich Klieger professorial chair of Chemical Physics.

Supporting Information Available: Measurements with P123-NO spin probe, PEO-NO in MWNT dispersions, and Arrhenius plot of τ_c temperature dependence in solutions of 4HTB in aqueous dispersions of SWNT (0.5 wt %) in P123 (1 wt %). This material is available free of charge via the Internet at <http://pubs.acs.org>.

References and Notes

- Iijima, S. *Nature* **1991**, *354*, 56.
- Sung, J. H.; Kim, H. S.; Jin, H.-J.; Choi, H. J.; Chin, I.-J. *Macromolecules* **2004**, *37*, 989.
- Kim, H. S.; Jin, H.-J.; Myung, S. J.; Kang, M.; Chin, I.-J. *Macromol. Rapid Commun.* **2006**, *27*, 146.
- Moore, V. C.; Strano, M. S.; Haroz, E. H.; Hauge, R. H.; Smalley, R. E. *Nano Lett.* **2003**, *3*, 1379–1382.
- Szleifer, I.; Yerushalmi-Rozen, R. *Polymer* **2005**, *46*, 7803.
- Shin, H. I.; Min, B. G.; Jeong, W. Y.; Park, C. *Macromol. Rapid Commun.* **2005**, *26*, 1451–1457.
- Yerushalmi-Rozen, R.; Bounioux, C.; Szleifer, I. *Chemistry of Carbon Nanotubes*; Basiuk, V. A., Basiuk, E. V., Eds.; American Scientific Publishers: Valencia, CA, 2008; pp 1–12.
- Wanka, G.; Hoffman, H.; Ulbricht, W. *Macromolecules* **1994**, *27*, 4145–4159.
- Alexandridis, P.; Lindman, B. *Amphiphilic Block Copolymers: Self-Assembly and Applications*; Elsevier: Amsterdam, 2000.
- Zhang, D.; Carignano, M. A.; Szleifer, I. *Phys. Rev. Lett.* **2006**, *028701*.
- Shvartzman-Cohen, R.; Florent, M.; Goldfarb, D.; Szleifer, I.; Yerushalmi-Rozen, R. *Langmuir* **2008**, *24*, 4625–4632.
- Florent, M.; Shvartzman-Cohen, R.; Goldfarb, D.; Yerushalmi-Rozen, R. *Langmuir* **2008**, *24*, 3773.
- Talmon, Y. In *Cryo Techniques in Biological Electron Microscopy*; Steinbrecht, R. A., Zierold, K., Eds.; Springer-Verlag: Berlin, 1987.
- Nativ-Roth, E.; Shvartzman-Cohen, R.; Bounioux, C.; Florent, M.; Zhang, D.; Szleifer, I.; Yerushalmi-Rozen, R. *Macromolecules* **2007**, *40*, 3676–3685.
- Mortensen, K.; Talmon, Y. *Macromolecules* **1995**, *28*, 8829–8834.
- Zhou, W.; Islam, M. F.; Wang, H.; Ho, D. L.; Yodh, A. G.; Winey, K. I.; Fischer, J. E. *Chem. Phys. Lett.* **2004**, *384*, 185–189.
- Dror, Y.; Pyckhout, H. W.; Cohen, Y. *Macromolecules* **2005**, *38*, 7828.
- Poncharal, P.; Wang, Z. L.; Ugarte, D.; de Heer, W. A. *Science* **1999**, *283*, 1513–1516.
- Schneider, D. J.; Freed, J. H. In *Spin Labelling: Theory and Applications*; Berliner, L. J., Reuben, J., Eds.; Biological Magnetic Resonance; Plenum: New York, 1989; Vol. 8, Chapter 1.
- Morisett, J. D. *Spin Labeling: Theory and Applications*; Academic Press: New York, 1976; Chapter 8.
- Lin, Y.; Alexandridis, P. *J. Phys. Chem. B* **2002**, *106*, 10834–10844.
- Carageorghopol, A.; Caldararu, H.; Dragutan, I.; Joela, H.; Brown, W. *Langmuir* **1997**, *13*, 6912–6921.
- Li, S.; Li, H.; Wang, X.; Song, Y.; Liu, Y.; Jiang, L.; Zhu, D. *J. Phys. Chem. B* **2002**, *106*, 9274–9276.
- Ruthstein, S.; Frydman, V.; Kababya, S.; Landau, M.; Goldfarb, D. *J. Phys. Chem. B* **2003**, *107*, 1739–1748.
- Ruthstein, S.; Frydman, V.; Goldfarb, D. *J. Phys. Chem. B* **2004**, *108*, 9016–9022.
- Shvartzman-Cohen, R.; Nativ-Roth, E.; Baskaran, E.; Levi-Kalishman, Y.; Szleifer, I.; Yerushalmi-Rozen, R. *J. Am. Chem. Soc.* **2004**, *126*, 14850–14857.
- Stone, T. J.; Buckman, T.; Nordio, P. L.; McConnell, H. M. *Proc. Natl. Acad. Sci. U.S.A.* **1965**, *54*, 1010–1017.
- Stoll, S.; Schweiger, A. *J. Magn. Reson.* **2006**, *178*, 42–55.
- Dormidontova, E. *Macromolecules* **2002**, *35*, 987–1001.
- In spite of ongoing efforts and application of different analytical methods, a reliable measure of the concentration of dispersed CNT has not been established. Different methods applied to a given sample provide significantly different values. See for example: WTEC Panel Report on International Assessment of Research and Development of Carbon Nanotube Manufacturing and Applications at <http://www.dtic.mil/cgi-bin/GetTRDoc?AD=A-DA472146&Location=U2&doc=GetTRDoc.pdf>.
- Ruthstein, S.; Schmidt, J.; Kesselman, E.; Popovitz-Biro, R.; Omer, L.; Frydman, V.; Talmon, Y.; Goldfarb, D. *Chem. Mater.* **2008**, *20*, 2779–2792.
- Wolff, T.; Weber, S.; Böhm, B.; Schütz, A. *Photochem. Photobiol.* **1995**, *62*, 82–86.